Performance enhancement of dye-sensitized solar cell by peripheral aromatic and heteroaromatic functionalization in di-branched organic sensitizers

Journal:	*New Journal of Chemistry*
Manuscript ID	NJ-ART-12-2017-005188
Article Type:	Paper
Date Submitted by the Author:	30-Dec-2017
Complete List of Authors:	Manfredi, Norberto; University of Milano-Bicocca, material science Trifiletti, Vanira; University of Milano-Bicocca, material science Melchiorre, Fabio; Eni S.p.A., Research Center for Non-Conventional Energies ISTITUTO ENI DONEGANI Giannotta, Giorgio; Eni S.p.A., Research Center for Non-Conventional Energies ISTITUTO ENI DONEGANI Biagini, Paolo; Eni S.p.A., Research Center for Non-Conventional Energies ISTITUTO ENI DONEGANI Abbotto, Alessandro; University of Milano-Bicocca, material science

SCHOLARONE™
Manuscripts

ARTICLE

Performance enhancement of dye-sensitized solar cell by peripheral aromatic and heteroaromatic functionalization in di-branched organic sensitizers

N. Manfredi,[*a†] V. Trifiletti,[a†] F. Melchiorre,[b] G. Giannotta,[b] P. Biagini,[*b] and A. Abbotto.[*a]

Di-branched dyes based on a triphenylamino (TPA) donor core have been functionalized with different aromatic and heteroaromatic peripheral groups bonded to TPA as auxiliary donors and investigated as sensitizers in DSSC. The different aromatic and heteroaromatic substitution significantly perturbed the optical properties of the dyes compared to the unsubstituted TPA reference dye, in turn leading to enhanced photovoltaic performances in terms of photocurrent, photovoltage, and power conversion efficiency (PCE). The enhancement originated from improved strategic interface interactions between dye-sensitized titania and the liquid electrolyte, as ascertained by current-voltage, quantum efficiency (IPCE), light harvesting properties (LHE), and impedance spectroscopy (EIS) studies.

Introduction

Since the pioneering report in 1991 by Grätzel and co-workers, dye-sensitized solar cells (DSSCs) have been receiving increasing interest due to their relatively high efficiency and low-cost fabrication.[1, 2] The dye-photosensitizer plays a strategic role in providing electron injection into the conduction band (CB) of TiO$_2$, upon light irradiation from Sun. The overall photoelectric power conversion efficiencies (PCE) of DSSCs, sensitised by metal complexes, have exceeded 12% at 1 sun irradiation intensity.[3] However, the limitations concerning these complexes, such as rare sources, heavy-metal toxicity and environmental issues, necessarily limit their broad application. In recent years, metal-free organic chromophores have been extensively investigated as alternative sensitizers to transition metal-complexes due to their high molar extinction coefficients, ease of structure tailoring, as well as low-cost synthesis processes, and compliance with environmental issues.[4] To date, hundreds of organic dyes have been explored to act as sensitizers for DSSCs and remarkable efficiencies, over 14%, have been obtained.[1, 5-10] Organic dyes possessing a rod-like configuration with the electron-donating and electron-

accepting groups, bridged by a π-spacer molecular system, are the most used. The most common donor moiety is a triphenylamine (TPA) derivative.[11, 12] This donor scaffold has been widely used in the synthesis of sensitizers, commonly bearing a long terminal alkoxy chain on peripherals phenyl rings[13] to reduce detrimental charge recombination or to enhance electron donation capabilities. A few years ago, we have proposed an innovative new molecular architecture for metal-free organic dyes based on a multi-branched geometry.[9] In that first report, we demonstrated that the new molecular architecture provides enhanced photoinduced intramolecular electron transfer, device photocurrent, stability under light and thermal stress. Furthermore, the photophysical properties of the multi-branched dyes can be widely tuned upon varying donor, spacer, and acceptor moieties; therefore, following our first report, significant numbers of studies have been reported on DSSC multi-branched dyes as sensitizers, showing the multiple advantages of this architecture. One of the most attractive reported features is the ability to show similar PCEs in both liquid and solid-state devices, unlike what occurs in the conventional linear geometry.[14] The most representative multi-branched structures, reported in the literature, and their studies in DSSC have been recently reviewed.[15]

Based on our previous work we decided to modify specific structural characteristics of di-branched dyes, mainly aimed to improve the critical interface between dye-decorated TiO$_2$ and the liquid electrolyte, to design a sensitizer class able to provide high performances also in large area DSSCs. Indeed, the electron recombination from TiO$_2$ to the oxidised form of the electrolyte represents one of the major drawbacks of the present device architecture and it is responsible for lower photovoltage, fill factor and, eventually, PCE.[16-20] Electron recombination is conveniently investigated via Electrochemical

a. Department of Materials Science and Milano-Bicocca Solar Energy Research Center – MIB-Solar, University of Milano-Bicocca, Via Cozzi 55, I-20125 Milano, Italy.

b. Research Center for Renewable Energy & Enviromental Istituto Donegani, Eni S.p.A., via Fauser 4, I-28100, Novara, Italy.

† These two authors contributed equally to the work.

Impedance Spectroscopy (EIS), which is able to determine the recombination resistance between TiO_2 and the electrolyte, in addition to other parameters related to the electron lifetime in the semiconductor.[21-23] One of the most effective strategies to limit charge recombination is to make the approach of the liquid electrolyte to the semiconductor surface more difficult by chemical modification of the dye.

Here we present a new family of DSSC di-branched sensitizers where the terminal donor TPA core has been functionalized with a (hetero)aromatic substituent (Ar) to affect the electrolyte-TiO_2 interaction. We have selected thieno[3,2-*b*]thiophene (TT) as a spacer previously used in efficient DSSC sensitizers,[13] and the conventional cyanoacrylic acid as double anchoring points.

Fig. 1 depicts the general design of the series Ar-TPA-[TT-anchoring]$_2$ investigated in this work. As our study focuses on the fundamental understanding of dye working principles, with no aspiration of obtaining high photovoltaic (PV) efficiencies, DSSCs are realized with the aim of simplifying the architecture and, therefore, the study of the interface phenomena: PCE up to 6.3% have been reached in conventional liquid iodine-based cells, based on a transparent TiO_2 monolayer and drop-casted Pt counter electrode.
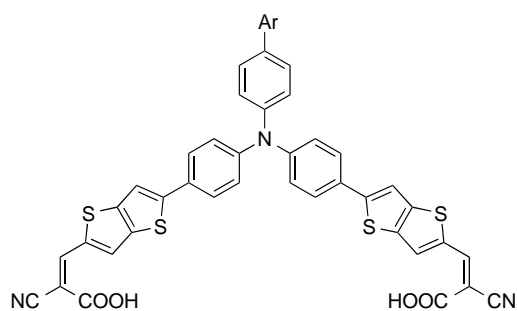

Fig. 1 General design of di-branched dyes with peripheral substitution on triphenylamino donor core to induce additional properties.

Results and discussion

Design and synthesis

Following the introduced general design strategy of Fig. 1, we have investigated the new dyes **TT-b-01** – **TT-b-03**. With the aim to investigate the peripheral substitution, pristine derivative TT-b-00 has been also prepared and characterized as a reference dye (Fig. 2). The TPA moiety of **TT-b-00** has been functionalized with thiophene-based substituents in **TT-b-01** and **TT-b-02** and with a benzene derivative in **TT-b-03**. The thiophene rings in **TT-b-01** and **TT-b-02** were further modified, according to the literature, with the introduction of a *n*-hexyl chain in the terminal free α-positions, in order to minimize charge recombination.[24-26] We selected 2,4-bis-hexyloxybenzene as a benzene derivative in **TT-b-03**. This group has been demonstrated to be an efficient surface protector via steric hindrance, regardless of the presence of co-adsorbents during dye adsorption on the semiconductor surface.[14] Both the

alkylthiophene and the bis-alkoxybenzene moieties allow further extension of the molecular π-framework and provide an auxiliary electron-rich donor contribution, so to enforce the electron-donating ability of the terminal moiety. These features can be exploited to enhance optical and electronic properties of the dyes, by improving light-harvesting abilities and better promoting the photo-induced intermolecular charge transfer (ICT) step preceding electron injection to TiO_2. The choice of the thieno[3,2-*b*]thiophene as a π-spacer was justified by an optimal trade-off between PV efficiency, as suggested by the literature,[13] and ease of synthesis.
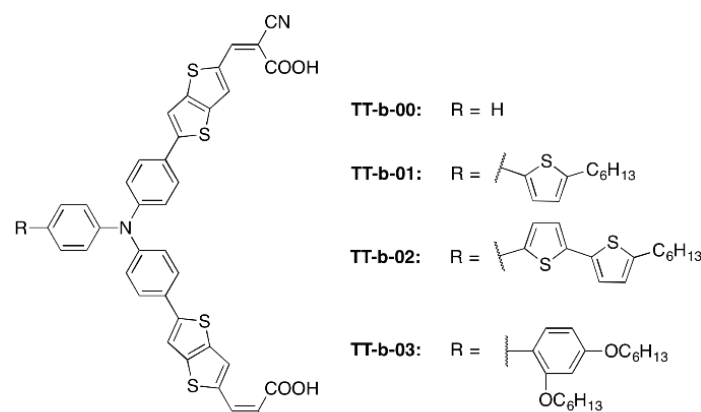

Fig. 2 **TT-b** dyes investigated in this work.

The reference dye **TT-b-00** has been synthesized according to Scheme 1. 4,4'-dibromotriphenylamine (**1**)[27] has been submitted to a Suzuki-Miyaura coupling with 4,4,5,5-tetramethyl-2-thieno[3,2-b]thiophen-2-yl-[1,3,2]dioxaborolane[28] in presence of a Pd(II) catalyst and a base to give the bis-thieno[3,2-*b*]thiophene branched intermediate **2**. Formylation under Vilsmeier-Haack conditions led to the key intermediate bis-aldehyde **3**, as a pure product, in moderate yields after precipitation from the crude reaction mixture. This compound is sparingly soluble in common organic solvent. Final condensation with cyanoacetic acid afforded the reference compound **TT-b-00** in good yields and, in contrast to its precursor, the final product is endowed with good solubility properties.

The synthetic access to the dyes **TT-b-01** – **TT-b-03** implies the use of the common TPA intermediate **3**, followed by the peripheral functionalization of TPA with the aromatic substituent, via a bromo-derivative **4**, and the final insertion of the electron-withdrawing-anchoring group (Scheme 2). The Suzuki-Miyaura coupling has been again selected as a convenient, sustainable and up-scalable method to introduce the different aromatic and heteroaromatic end-groups. In the case of the thiophene-based derivatives, the boronic esters were commercially available. The proper boronic ester for the insertion of the 2,4-dihexyloxyphenyl substituent has been prepared according to the literature.[29] Once the derivatized bis-aldehydes **5a** – **c** has been obtained, the final condensation, similarly to the reference dye, afforded the desired products.
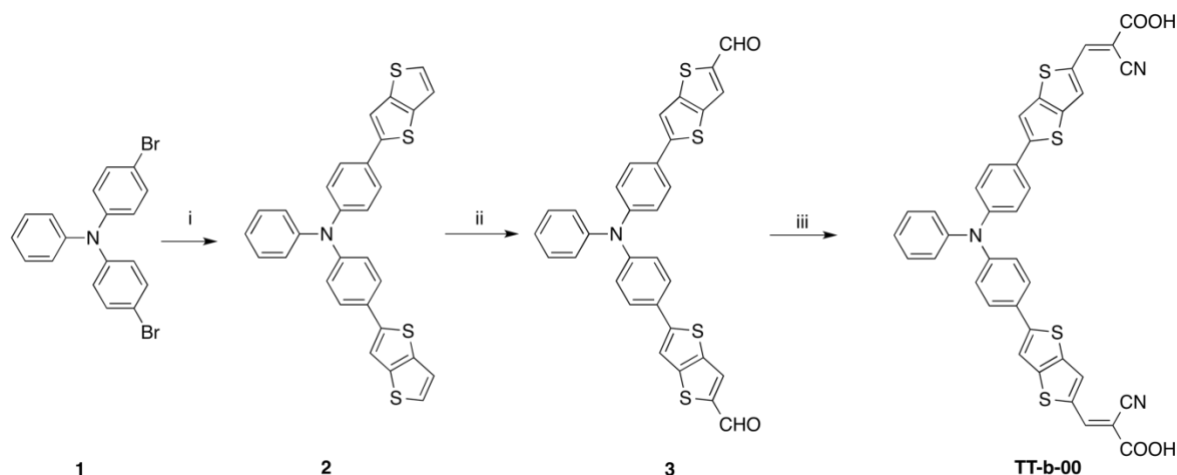
Scheme 1 Synthetic strategy for the reference compound **TT-b-00**. i) 4,4,5,5-tetramethyl-2-thieno[3,2-b]thiophen-2-yl-[1,3,2]dioxaborolane, Pd(dppf)Cl$_2$, K$_2$CO$_3$, MeOH, toluene, 70°C, microwaves; ii) POCl$_3$, DMF, N$_2$, 0 °C to 70 °C; iii) CNCH$_2$COOH, CHCl$_3$, reflux.
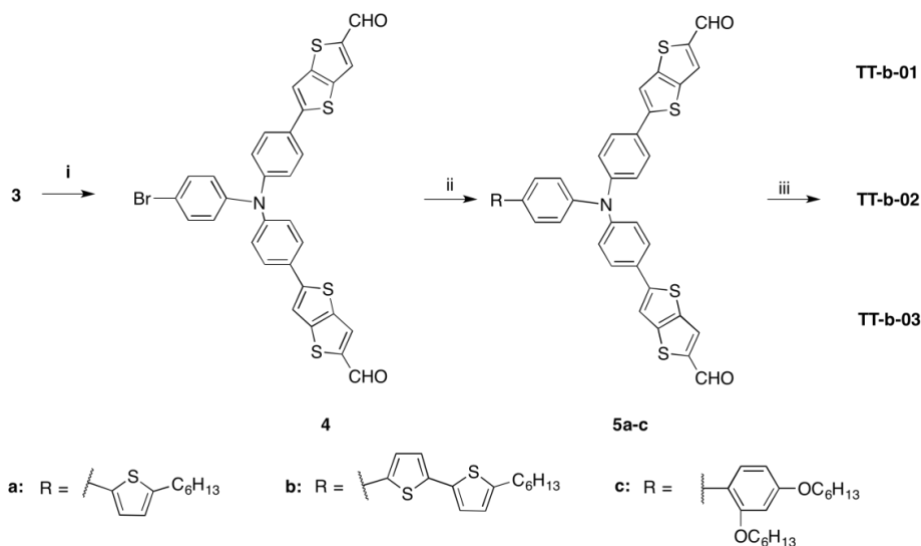
Scheme 2 Synthesis of the enforced donor **TT-b** dyes. i) NBS, DMF, 0 °C to rt; ii) aryl boronic derivatives, Pd(dppf)Cl$_2$, K$_2$CO$_3$, MeOH, toluene, 70°C, microwaves; iii) CNCH$_2$COOH, CHCl$_3$, reflux.

Optical and Electrochemical characterization

The optical characterizations of the dyes **TT-b-00** - **TT-b-03** were performed in 10^{-5} M EtOH solutions. Absorption spectra normalised to molar extinction coefficients (ε) are shown in Fig. 3 and the relevant values collected in Table 1. All the dyes showed a typical pattern of donor-acceptor chromophores, with an intense ICT absorption band in the Vis region.

The introduction of the auxiliary aromatic electron-rich fragments on the donor TPA moiety led to a substantial qualitative and quantitative enhancement of the optical properties compared to the reference **TT-b-00**. A bathochromic effect has been observed moving from the unsubstituted derivative to **TT-b-01** and **TT-b-02**. A stronger effect was recorded upon insertion of the 2,4-dialkoxyphenyl group, with a red shift of more than 20 nm. A similar behaviour upon derivatization of **TT-b-00** has been observed in the trend of the molar absorptivity. The hyperchromic effect induced by the

aromatic substitution of the TPA core increased the ε value from 44 000 to over 60 000 M^{-1} cm^{-1} in the 2,4-dihexyloxyphenyl derivative **TT-b-03**, corresponding to an enhancement of nearly 50%.

Notably neither a bathochromic nor a hyperchromic effect has been observed upon increasing the number of thienyl rings of the aromatic terminal substituent, with the only marginal difference residing in the pattern at higher energies, likely due to local transitions. The emission spectra have been qualitatively determined and illustrated in comparison with absorption properties in Fig. S1 (see ESI). The zeroth-zeroth transition energies (E$_{0-0}$) have been estimated from the intercept of the normalised absorption and emission spectra in the same solvent and the values collected in Table 1.
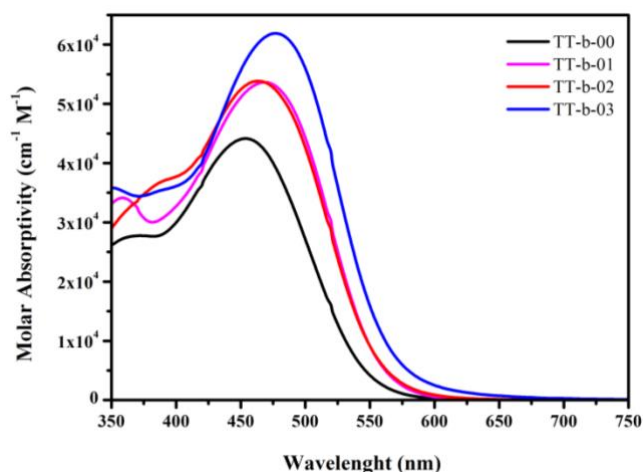
Fig. 3 Absorption spectra of dyes **TT-b-00** - **TT-b-03** in EtOH.

Saturated solutions of **TT-b** dyes in DMF (< 10^{-4} M) were used for the electrochemical characterization by dissolving each compound in the supporting electrolyte (0.1 M TBABF$_4$). The main electrochemical and energetic parameters have been collected in Table 1. The cyclic voltammetry (CV) study (Fig. S2, ESI) showed an irreversible behavior at oxidative potentials (potential > 0 V) for all the dyes due to precipitation of the oxidized compounds. HOMO/LUMO energies referred to vacuum,[30] are pictorially depicted in Fig. 4 as well as the energy level of the CB of TiO$_2$.[31]

The oxidative processes showed a first oxidation wave spanning from 200 to 310 mV vs Fc/Fc$^+$. In general, the presence of the different thienyl or phenyl ring substituents on the triarylamino donor core did not significantly affect the oxidation potential of the dyes. Accordingly, the HOMO energy levels were almost similar in the **TT-b** series. LUMO energies were calculated from the electrochemical HOMO energies by using the optical bandgaps, as measured as onset energies by means of the Tauc plot.[32]
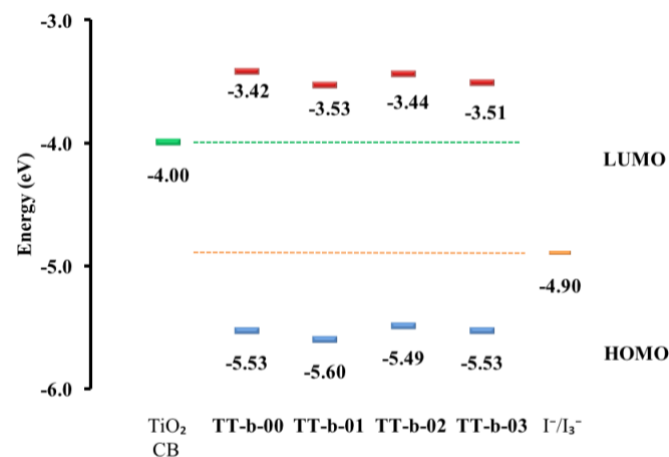

Fig. 4 Scheme of the energy levels of the investigated dyes compared to the CB of TiO$_2$.

Table 1 Optical and electrochemical characterization of dyes **TT-b-00** - **TT-b-03** in solution.

dye	λ_{max} abs[a] (nm)	ε (cm^{-1} M^{-1})	λ_{max} em[a] (nm)	E_{0-0} (eV)	E_{ox} (V vs Fc/Fc$^+$) ± 10 mV	HOMO[c] (eV) ± 100 meV	E_{gap}^{opt} (eV)	LUMO[c] (eV) ± 100 meV
TT-b-00	454	44 100 ± 350	587	2.39	0.24	-5.53	2.11	- 3.42
TT-b-01	469	53 700 ± 430	610	2.32	0.31	-5.60	2.07	- 3.53
TT-b-02	463	53 900 ± 370	610	2.34	0.20	-5.49	2.05	- 3.44
TT-b-03	477	61 900 ± 380	635	2.28	0.24	-5.53	2.02	- 3.51

[a] 10^{-5} M solution in EtOH; [b] saturated solution in supporting electrolyte (0.1 M TBABF$_4$ in DMF); [c] Vacuum potential = Fc/Fc$^+$ + 5.29 V.

Photovoltaic Investigation

To better compare the PV properties of the new dyes, we have employed **TT-b-00 – TT-b-03** as sensitizers in single layer DSSCs. By using a single transparent semiconductor layer only one titania interface is present, simplifying the interface phenomena. Furthermore, without the opaque scattering layer, a complete optical and electrochemical characterization could be performed on the same devices used for the PV investigation. However, it should be noted that the absence of a scattering layer does not allow to reach optimal photocurrent values and thus the obtained PCEs should be considered as minimal values with respect to full optimization, which was not the main scope of this work. [2, 33]

DSSCs were fabricated using a screen-printed transparent 9-μm monolayer film consisting of 20-nm TiO$_2$ particles (Dyesol 18NR-T). The active area of the device was 0.20 cm^2. The PV response of the devices has been investigated by varying the amount of

chenodeoxycholic acid (CDCA) as a de-aggregating co-adsorbent agent in the sensitizer solution,[34] finding that the most favourable results are obtained by using an equimolar amount of dye and CDCA (Table S1, see ESI). The best average PCE were measured using the electrolyte Z960 (1.0 M 1,3-dimethylimidazolium iodide, 0.03 M I$_2$, 0.05 M LiI, 0.10 M guanidinium thiocyanate, and 0.50 M 4-t-butylpyridine in acetonitrile/valeronitrile 85:15).[35] Main PV parameters of the new dyes are listed in Table 2 together with those of the reference benchmark dye N719, used as a sensitizer in the control device. PV measurements of DSSCs were carried out with a black metal mask with an aperture area of 0.28 cm^2 to avoid current overestimation due to multiple irradiation.[36] The overall conversion efficiencies PCE were derived from the equation: PCE = J_{sc} x V_{oc} x FF, where J_{sc} is the short circuit current density, V_{oc} the open circuit voltage, and FF the fill factor.

Fig. 5 shows the photocurrent-voltage curves of DSSCs. The control **N719**-sensitized device guaranteed the reliability of the

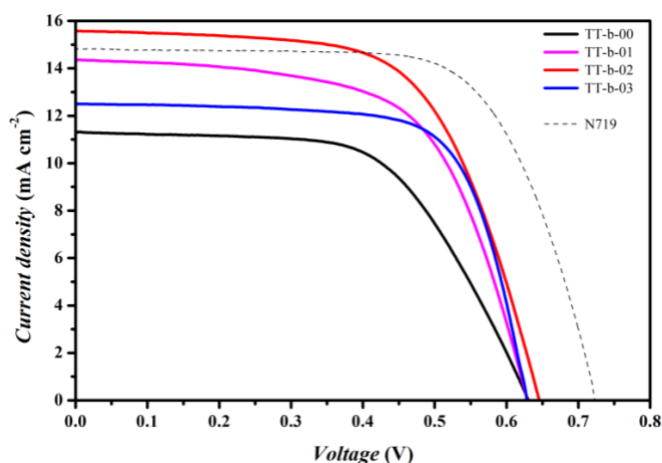production process, with its PCE agreeing with best routine literature values based on monolayer cells.

Fig. 5 Current–voltage characteristics of DSSCs sensitised by **TT-b-00** - **TT-b-03** in comparison with the control cell sensitised by benchmark **N719**.

Table 2 Main PV parameters of DSSCs based on the di-branched sensitizers **TT-b-00** – **TT-b-03** in comparison with the benchmark **N719**.

dye	J_{sc} (mA cm^{-2})	V_{oc} (mV)	FF	PCE (%)
TT-b-00[a]	11.3	629	0.60	4.3
TT-b-01[a]	14.3	628	0.62	5.6
TT-b-02[a]	15.6	645	0.62	6.3
TT-b-03[a]	12.5	627	0.71	5.5
N719[b]	14.8	724	0.68	7.3

[a] Dye solution: 2 x 10^{-4} M in EtOH + 2 x 10^{-4} M CDCA; [b] dye solution: 5 x 10^{-4} M in EtOH + 5 x 10^{-4} M CDCA.

The effect of the substitution on the donor TPA moiety is evident. Measured photocurrent values are larger for **TT-b-01** - **TT-b-03** compared to **TT-b-00**, in agreement with the superior optical properties of the former dyes. The highest values have been measured for the bithienyl derivatives, **TT-b-02** showing a current even larger than that of the device based on **N719**. Photovoltages are similar for all the devices and lower than that of the **N719**-based cell. The good current value for **TT-b-02** led to a PCE larger than 6%, which is mid-high ranked in the literature for DSSC based on a single TiO$_2$ layer [33] and very close to the control **N719** device, compared to which the PCE is only ~15% less intense.

The incident monochromatic photon-to-current conversion efficiencies (IPCE, 0-100%) of the investigated DSSCs are shown in Fig. 6. The IPCE data agree with the current/voltage measurements. The **TT-b-02** device showed the most intense external quantum efficiency, with a maximum value of ~ 90% in the 500 – 550 nm region.

For a more detailed understanding of the different PV performances registered for the phenyl- and thienyl-modified derivatives, we have separately examined the two constituting factors of IPCE, per equation IPCE(λ) = LHE(λ) x APCE(λ) (Fig. 7). LHE (0-100%) is the light-harvesting efficiency and is associated with the ability of the cell to harvest light. APCE (0-100%) is the absorbed monochromatic photon-to-current conversion efficiency and gives the internal quantum efficiency of the cell in generating electric current, being related to the electron injection efficiency from the dye to the semiconductor oxide, the dye regeneration efficiency, and the charge collection efficiency.[37, 38] IPCE and LHE (LHE=1-10^{-Abs}) are experimentally determined. APCE is thus derived by dividing the IPCE number by LHE. LHE, and indirectly APCE, can be measured only for transparent dye-coated films, as similarly performed for previous representative studies,[3, 39-42] since scattering layers do not allow the use of quantitative absorption spectroscopy.
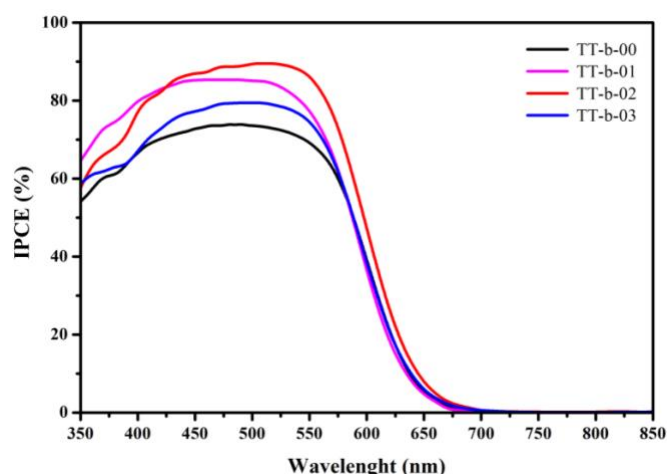

Fig. 6 IPCE of DSSCs sensitised by **TT-b-00** - **TT-b-03**.

In this respect, we justify our choice to use here single layer devices that, while not being associated with optimum PCE, allow us to study in detail the devices in all their most important components and effectively complete the comparative design study for the different sensitizers. Fig. 7 shows the LHE spectra of the sensitized photoanodes in **TT-b-01** - **TT-b-03** based DSSCs. The comparison between the three dyes clearly shows how the thienyl based devices have a higher light harvesting ability than that of the phenyl derivative, despite the latter dye presents in solution the best optical properties. Therefore, the absorption investigation in the device, LHE, fully justifies the higher value of photocurrent observed for the compound **TT-b-02**. It is evident that APCE (inset of Fig. 7) is excellent for almost the entire range of visible light. **TT-b-02** extends the range of maximum performance compared to **TT-b-01**. The best combined performance of electron injection, dye regeneration, and charge collection efficiency has been recorded for **TT-b-03**, as confirmed by the best cell FF (Table 2). Therefore, the phenyl derivative is the most efficient dye in terms of the conversion efficiency of absorbed photons. Unfortunately, the lower light harvesting efficiency negatively counterbalances this performance decreasing the cell current and, eventually, device PCE.
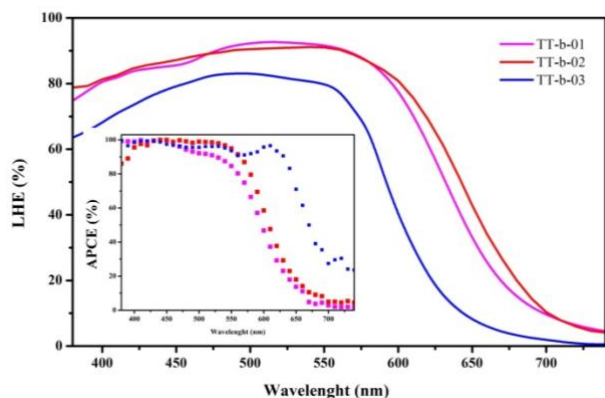
Fig. 7 LHE and APCE (inset) of the photoanodes sensitised by **TT-b-01 - TT-b-03**.

For a more detailed comparative investigation, we decided to use EIS and focus attention on charge recombination phenomena.[21-23] In this experiment, a small sinusoidal voltage stimulus of a fixed frequency is applied to an electrochemical cell and its current response measured. The behaviour of an electrochemical system can be investigated by sweeping the frequency over several orders of magnitude (generally from a few mHz to several MHz). The analysis of the impedance spectra was performed in terms of Nyquist plots (Fig. 8), where the imaginary part of the impedance is plotted as a function of the real part of the range of frequencies. Under soft illumination (0.25 sun), at open circuit voltage conditions, the properties of the sensitized TiO_2/electrolyte interface can be derived from the Nyquist plot in terms of recombination resistance (R_{rec}) and chemical capacitance (C_μ), which have been obtained by fitting the data with the equivalent circuit reported in the inset of the Figure. The apparent electron lifetime τ_n can be calculated from $\tau_n = R_{rec} \times C_\mu$.[21, 43] The results of the EIS investigation are summarised in Table 3. These data reveal that corresponding capacitances, which probe the charge carrier accumulation in the TiO_2 film and the density of states in the band gap, resulted identical for all the dyes.

Table 3 Parameters calculated from EIS data plots of DSSCs based on **TT-b-01** and **TT-b-02**.

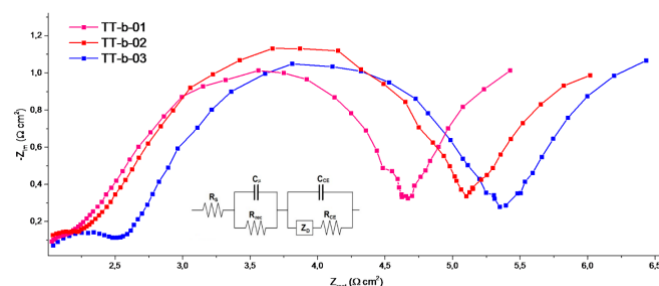| Dye	R_{rec} (Ω cm^2)	C_μ (F cm^{-2})	τ_n (ms)
TT-b-01	1.8	1.1×10^{-3}	1.9
TT-b-02	2.2	1.1×10^{-3}	2.3
TT-b-03	2.7	1.1×10^{-3}	3.0

Fig. 8 EIS data plots of DSSCs sensitised by **TT-b-01** - **TT-b-03**.

As previously reported,[44] minor changes of the chemical structure, which can affect the performance of the device despite the unvaried optical properties, suggest that the effect on the recombination resistance is more relevant important than that on the capacitance.

Indeed, **TT-b-01** and **TT-b-02** have been found to be optically almost equivalent, both in solution and when adsorbed on titania, meanwhile **TT-b-03** shows poor light harvesting capability when it is anchored on the titania substrate, even if it shows the longest electron lifetime. **TT-b-01** and **TT-b-03** based devices afforded similar photovoltages, since this depends on the saturation current density, associated to charge recombination, and on the photogenerated current. [45] Dye **TT-b-01** shows a higher current and a lower R_{rec}, whereas **TT-b-03** shows a lower generated current and a higher R_{rec}. The good recombination resistance and the high light harvesting efficiency of the **TT-b-02** device justifiy the higher PV response. This trend supports an effective suppression of the back reaction of the injected electrons with the electrolyte for **TT-b-02** and an excellent energy harvesting, which leads to a larger photocurrent and photovoltage[21, 22] and, accordingly, to the best PCE of the series.

Conclusions

In summary, we synthesised a new series of di-branched dyes based on a TPA donor core functionalized with different peripheral auxiliary donor groups. The new dyes were investigated as sensitizers in DSSCs. We focused on the effect of the peripheral groups bonded to TPA: we found a more effective suppression of the back reaction involving the injected electrons and the electrolyte for the two thienyl derivatives, thus suggesting an enhanced photoinduced intramolecular electron transfer.

The superior performance showed by the **TT-b-02** dye, supported by current-voltage, IPCE, LHE, and EIS data, arises from an improved interface interaction between dye-sensitized TiO_2 and the liquid electrolyte. We thus believe that the new dyes might provide an important design strategy to improve general performances in large area DSSCs of industrial relevance, a sector where the critical interface between the optically active layer and the electrolyte is still a challenging issue.

Experimental section

Materials and methods

NMR spectra were recorded with a Bruker AMX-500 spectrometer operating at 500.13 MHz (^{1}H) and 125.77 MHz (^{13}C). Coupling constants are given in Hz. Absorption spectra were recorded with a V-570 Jasco spectrophotometer. Emission spectra were recorded with a FP-6200 Jasco spectrofluorometer. Flash chromatography was performed with Merck grade 9385 silica gel 230–400 mesh (60 Å). Reactions performed under inert atmosphere were done in oven-dried glassware and a nitrogen atmosphere was generated with Schlenk technique. Conversion was monitored by thin-layer chromatography by using UV light (254 and 365 nm) as a visualizing agent. All reagents were obtained from commercial suppliers at the highest purity grade and used without further purification. Anhydrous solvents were purchased from Sigma-Aldrich and used without further purification. Extracts were dried with Na_2SO_4 and filtered before removal of the solvent by evaporation. 4,4'-dibromotriphenylamine and 4,4,5,5-tetramethyl-2-thieno[3,2-b]thiophen-2-yl-[1,3,2]dioxaborolane have been synthesized according to literature.[27,28]

Cyclic Voltammetry (CV) was carried out at scan rate of 100 mV/s, using a PARSTA2273 potentiostat in a three electrode electrochemical cell under Ar. The working, counter, and the pseudo-reference electrodes were a glassy carbon pin, a Pt wire and an Ag/AgCl wire, respectively. The working electrodes discs were well polished with alumina 0.1 µm suspension. The Pt wire was sonicated for 15 min in deionized water, washed with 2-propanol, and cycled for 50 times in 0.5 M H_2SO_4 before use. The Ag/AgCl pseudo-reference electrode was calibrated, by adding ferrocene (10^{-3} M) to the test solution after each measurement.

The following materials were purchased from commercial suppliers: FTO-coated glass plates (2.2 mm thick; sheet resistance ~7 ohm per square; Solaronix); Dyesol 18NR-T transparent TiO_2 blend of active 20 nm anatase particles; N719 (Sigma-Aldrich). UV-O_3 treatment was performed using Novascan PSD Pro Series – Digital UV Ozone System. The thickness of the layers was measured by means of a VEECO Dektak 8 Stylus Profiler. PV measurements of DSSCs were carried out with an antireflective layer and with black metal mask on top of the photoanode of 0.28 cm^2 surface area under a 500 W Xenon light source (ABET Technologies Sun 2000 class ABA Solar Simulator). The power of the simulated light was calibrated to AM 1.5 (100 mW cm^{-2}) using a reference Si cell photodiode equipped with an IR-cutoff filter (KG-5, Schott) to reduce the mismatch in the region of 350-750 nm between the simulated light and the AM 1.5 spectrum. I–V curves were obtained by applying an external bias to the cell and measuring the generated photocurrent with a Keithley model 2400 digital source meter. Incident photon-to-current conversion efficiencies (IPCE) were recorded as a function of excitation wavelength by using a monochromator (Omni 300 LOT ORIEL) with single grating in Czerny-Turner optical design, in AC mode with a chopping frequency of 1 Hz and a bias of blue light (0.3

sun). Absorption spectra were recorded on a V-570 Jasco spectrophotomer. EIS spectra were obtained using an Eg&G PARSTAT 2263 galvanostat potentiostat. The measurements have been performed in the frequency range from 100 kHz to 0.1 Hz under AC stimulus with 10 mV of amplitude and no applied voltage bias. The obtained Nyquist plots have been fitted via a non-linear least square procedure using the equivalent circuit model depicted in the inset of the plot itself.

Synthesis

Phenyl-bis-(4-thieno[3,2-b]thiophen-2-yl-phenyl)-amine, 2. Bis-(4-bromo-phenyl)-phenyl-amine (2.0 g, 4.96 mmol), was dissolved in methanol/toluene (1/1 v/v, 50 mL), then 4,4,5,5-tetramethyl-2-thieno[3,2-b]thiophen-2-yl-[1,3,2]dioxaborolane (3.3 g, 12.4 mmol), K_2CO_3 (3.43 g, 24.8 mmol) and Pd(dppf)Cl$_2$ (405 mg, 0.50 mmol) were added. The reaction mixture was heated at 70 °C for 2 h under µw irradiation (100 W). The mixture was diluted with NH_4Cl (sat. sol., 100 mL), the two layers were separated and the aqueous layer was extracted with CH_2Cl_2 (3 x 50 mL). The combined organic layers were washed with H_2O (50 mL), dried over Na_2SO_4 and then the solvent was removed under reduced pressure. The crude was purified by flash chromatography (petroleum ether/ethyl acetate 9/1) yielding phenyl-bis-(4-thieno[3,2-b]thiophen-2-yl-phenyl)-amine (**2**) (1.22 g, 47 %) as yellow solid. ^{1}H-NMR (500MHz, CDCl$_3$): δ_H 7.52 (d, J = 8.7 Hz, 4H), 7.41 (s, 1H), 7.34 (d, J = 5.2 Hz, 1H), 7.31 (d, J = 7.5 Hz, 1H), 7.25 (d, J = 5.1 Hz, 1H), 7.18 (d, J = 7.6 Hz, 1H), 7.13 (d, J = 8.6 Hz, 2H), 7.10 (t, J = 6.9 Hz, 1H).

5,5'-((phenylazanediyl)bis(4,1-phenylene))bis(thieno[3,2-b]thiophene-2-carbaldehyde), 3. In a two neck flask under nitrogen, freshly distilled POCl$_3$ (138 mg, 0.9 mmol) was added to anhydrous DMF (65 mg, 0.9 mmol) at 0 °C. The reaction mixture was kept at 0 °C for 30 min until the formation of a transparent glassy solid has been observed. Then, anhydrous DMF (10 mL) was added and the reaction and the mixture were allowed to warm to room temperature. A solution of phenyl-bis-(4-thieno[3,2-b]thiophen-2-yl-phenyl)-amine (**2**) (200 mg, 0.39 mmol) in anhydrous DMF (10 mL) was added to the reaction mixture, and then heated at 70 °C for 4 h. The reaction mixture was then poured in water saturated with CH_3COONa (100 mL) and stirred for 1 h. AcOEt (30 mL) was added and the organic phase was separated, and the aqueous phase extracted with AcOEt (2 x 30 mL).The collected organic phase was dried over Na_2SO_4, filtered and the solvent evaporated under reduced pressure yielding an orange oil. Et$_2$O was then added to the oil and 5,5'-((phenylazanediyl)bis(4,1-phenylene))bis(thieno[3,2-b]thiophene-2-carbaldehyde) (**3**) was obtained as an orange solid (171 mg, 0.29 mmol, yield 76 %) not much soluble in most of the organic solvent. ^{1}H NMR (500 MHz, DMSO) δ 9.98 (s, 2H), 8.40 (s, 2H), 7.94 (s, 2H), 7.72 (d, J = 8.7 Hz, 3H), 7.42 (d, J = 8.4 Hz, 2H), 7.22 (d, J = 7.5 Hz, 1H), 7.18 (d, J = 7.5 Hz, 2H), 7.13 (d, J = 8.7 Hz, 4H).

TT-b-00. Intermediate **3** (70 mg, 0.12 mmol) was suspended in CHCl$_3$ (10 mL). Cyanoacetic acid (103 mg, 1.21 mmol) and piperidine (113 mg, 1.33 mmol) were added and the mixture was refluxed for 8 h. The mixture was concentrated and 10%

HCl aqueous solution (40 mL) was added, then it was filtered and the solid was washed with H_2O (100 mL). **TT-b-00** (62 mg, 72 %) was recovered as red solid. ^1H-NMR (500 MHz, DMSO): δ_H 13.72 (bs, 2H), 8.58 (s, 2H), 8.33 (s, 2H), 7.98 (s, 2H), 7.72 (d, J = 8.7Hz, 4H), 7.42 (t, J = 7.8Hz, 2H), 7.23-7.18 (m, 3H), 7.14 (d, J = 8.7Hz, 4H). Elem. Anal. Calcd. for $C_{38}H_{21}N_3O_4S_4 \bullet 5H_2O$: C 56.92%, H 3.90%, N 5.24%; found C 57.32%, H 3.82%, N 5.44%.

5,5'-(((4-bromophenyl)azanediyl)bis(4,1-phenylene))bis(thieno[3,2-b]thiophene-2-carbaldehyde) 4. Dialdheyde **3** (100 mg, 0.17 mmol) was suspended in DMF (5 mL). The mixture was cooled to 0 °C, then a solution of NBS (31 mg, 0.17 mmol) in DMF (5 mL) was added dropwise and the reaction mixture was allowed to warm to room temperature overnight. The solution was diluted with water (100 mL) and filtered, then washed with water (100 mL). Compound **4** (120 mg, 100 %) was recovered as brown solid. ^1H NMR (500 MHz, DMSO) δ 9.97 (s, 2H), 8.40 (s, 2H), 7.95 (s, 2H), 7.73 (d, *J* = 8.7 Hz, 4H), 7.55 (d, *J* = 8.8 Hz, 2H), 7.15 (d, *J* = 8.7 Hz, 4H), 7.10 (d, *J* = 8.8 Hz, 2H). ^{13}C-NMR (500 MHz, DMSO): δ_c 185.89, 152.89, 148.29, 147.33, 146.83, 145.21, 138.96, 134.04, 132.81, 129.59, 128.65, 128.08, 125.41, 117.52, 117.41.

5,5'-(((4-(5-hexylthiophen-2-yl)phenyl)azanediyl)bis(4,1-phenylene))bis(thieno[3,2-b]thiophene-2-carbaldehyde), 5a. **4** (100 mg, 0.15 mmol) was dissolved in MeOH/toluene (1/1 *v/v*, 5 mL), then 5-hexyl-2-thiopheneboronic acid pinacol ester (90 mg, 0.30 mmol), Pd(dppf)Cl$_2$ (25 mg, 0.03 mmol) and K$_2$CO$_3$ (110 mg, 0.8 mmol) were added. The mixture was heated to 70 °C for 40 min under µw irradiation (70 W), then it was diluted with NH$_4$Cl (sat. sol. 50 mL). The aqueous layer was extracted with CH$_2$Cl$_2$ (3 x 20 mL), the organic layer was dried and the solvent was removed under reduced pressure. The crude was purified by flash chromatography (CH$_2$Cl$_2$) yielding the desired product **5a** as a dark orange solid (50 mg, 46%). ^1H NMR (500 MHz, CDCl$_3$) δ_H 9.94 (s, 2H), 7.89 (s, 2H), 7.56 (d, *J* = 8.6 Hz, 4H), 7.52 (d, *J* = 8.5 Hz, 2H), 7.46 (s, 2H), 7.18 (d, *J* = 8.6 Hz, 4H), 7.15 (d, *J* = 8.5 Hz, 2H), 7.09 (d, *J* = 3.5 Hz, 1H), 6.75 (d, *J* = 3.5 Hz, 1H), 2.82 (t, *J* = 7.6 Hz, 2H), 1.74 – 1.66 (m, 2H), 1.42-1.35 (m, 2H), 1.35-1.30 (m, 4H), 0.90 (t, *J* = 6.9 Hz, 3H). ^{13}C NMR (126 MHz, CDCl$_3$) δ_c 182.99, 152.63, 147.68, 147.01, 145.73, 145.16, 144.30, 140.84, 137.74, 131.08, 129.13, 128.34, 127.23, 126.62, 125.60, 125.09, 123.95, 122.48, 114.94, 31.58, 31.56, 30.25, 28.74, 22.55, 14.05.

5,5'-(((4-(5'-hexyl-[2,2'-bithiophen]-5-yl)phenyl)azanediyl)bis(4,1-phenylene))bis(thieno[3,2-b]thiophene-2-carbaldehyde), 5b. **4** (52 mg, 0.08 mmol) was dissolved in MeOH/toluene (1/1 *v/v*, 4 mL), then 5'-Hexyl-2,2'-bithiophene-5-boronic acid pinacol ester (75 mg, 0.2 mmol), Pd(dppf)Cl$_2$ (8 mg, 0.01 mmol) and K$_2$CO$_3$ (55 mg, 0.4 mmol) were added. The mixture was heated to 80 °C for 40 min under µw irradiation (50 W), then it was diluted with NH$_4$Cl (sat. sol. 20 mL). The aqueous layer was extracted with CH$_2$Cl$_2$ (3 x 20 mL), the organic layer was dried and the solvent was removed under reduced pressure. The crude was purified by flash chromatography (CH$_2$Cl$_2$) yielding the desired product **5b** as brown oil (30 mg, 50%). ^1H NMR (500 MHz, CDCl$_3$) δ 9.95 (s, 1H), 7.91 (s, 1H), 7.56 (dd, *J* = 15.6, 8.7 Hz, 3H), 7.48 (s, *J* = 2.3 Hz, 1H), 7.22 – 7.12 (m, 3H), 7.07 (d, *J* = 3.6 Hz, 1H), 7.01 (d, *J* = 3.5

Hz, 1H), 6.69 (d, *J* = 3.5 Hz, 1H), 2.80 (t, *J* = 7.6 Hz, 2H), 1.69 (m, 2H), 1.38 (m, 2H), 1.32 (m, 4H), 0.90 (t, *J* = 7.0 Hz, 3H).

5,5'-(((2',4'-bis(hexyloxy)-[1,1'-biphenyl]-4-yl)azanediyl)bis(4,1-phenylene))bis(thieno[3,2-b]thiophene-2-carbaldehyde), 5c. Compound **4** (100 mg, 0.15 mmol) was dissolved in MeOH/toluene (1/1 *v/v*, 7 mL), then 2,4-dihexyloxyphenylboronic acid pinacol ester (121 mg, 0.3 mmol), Pd(dppf)Cl$_2$ (25 mg, 0.03 mmol) and K$_2$CO$_3$ (110 mg, 0.8 mmol) were added. The mixture was heated to 70 °C for 60 min under µw irradiation (70 W), then it was diluted with NH$_4$Cl (sat. sol. 20 mL). The aqueous layer was extracted with CH$_2$Cl$_2$ (3 x 20 mL), the organic layer was dried and the solvent was removed under reduced pressure. The crude was purified by flash chromatography (CH$_2$Cl$_2$) yielding the desired product **5c** as a dark orange solid (87 mg, 66%). ^1H NMR (500 MHz, CDCl$_3$) δ_H 9.95 (s, 2H), 7.90 (s, 2H), 7.56 (d, *J* = 8.7 Hz, 4H), 7.52 (d, *J* = 8.6 Hz, 2H), 7.47 (s, 2H), 7.28 (s, 1H), 7.21 (d, *J* = 8.7 Hz, 4H), 7.18 (d, *J* = 8.5 Hz, 2H), 6.58 – 6.54 (m, 2H), 3.99 (m, 4H), 1.85 – 1.71 (m, 4H), 1,62-1,44 (m, 4H), 1.38-1.28 (m, 8H), 0.92 (t, *J* = 6.9 Hz, 3H), 0.88 (t, *J* = 7.0 Hz, 3H).

TT-b-01. **5a** (50 mg, 0.07 mmol) was dissolved in CHCl$_3$ (5 mL) then cyanoacetic acid (60 mg, 0.7 mmol) and piperidine (68 mg, 0.8 mmol) were added and the mixture was refluxed for 8 h. The mixture was concentrated and diluted with 10% HCl aqueous solution (30 mL). The formation of a precipitate was observed and, it was filtered under reduced pressure and washed with water (20 mL). The product **TT-b-01** was recovered as dark solid (30 mg, 50%). ^1H NMR (500 MHz, DMSO) δ_H 8.47 (s, 2H), 8.25 (s, 2H), 7.97 (s, 2H), 7.72 (d, *J* = 8.7 Hz, 4H), 7.60 (d, *J* = 8.6 Hz, 2H), 7.28 (d, *J* = 3.5 Hz, 1H), 7.16 (m, 6H), 6.84 (d, *J* = 3.5 Hz, 1H), 2.80 (t, *J* = 7.5 Hz, 2H), 1.69 – 1.59 (m, 2H), 1.39 – 1.26 (m, 6H), 0.88 (t, *J* = 7.0 Hz, 3H). Elem. Anal. Calcd. for $C_{48}H_{35}N_3O_4S_5 \bullet 2H_2O$: C 63.07%, H 4.30%, N 4.60%; found C 62.87%, H 4.47%, N 4.88%.

TT-b-02. **5b** (30 mg, 0.04 mmol) was dissolved in CHCl$_3$ (5 mL) then cyanoacetic acid (34 mg, 0.4 mmol) and piperidine (42 mg, 0.5 mmol) were added and the mixture was refluxed for 8 h. The mixture was concentrated and diluted with 10% HCl aqueous solution (20 mL). The formations of a precipitate were observed and filtered under reduced pressure and washed with water (20 mL). The product **TT-b-02** was recovered as dark solid (28 mg, 75%) ^1H NMR (500 MHz, DMSO) δ_H 8.56 (s, 2H), 8.31 (s, 2H), 7.99 (s, 2H), 7.74 (d, *J* = 8.6 Hz, 4H), 7.66 (d, *J* = 8.5 Hz, 2H), 7.43 (d, *J* = 3.7 Hz, 1H), 7.22 (d, *J* = 3.7 Hz, 1H), 7.21 – 7.15 (m, 6H), 7.14 (d, *J* = 3.7 Hz, 1H), 6.82 (d, *J* = 3.4 Hz, 1H), 2.79 (t, *J* = 7.4 Hz, 2H), 1.67 – 1.58 (m, 2H), 1.39 – 1.26 (m, 6H), 0.87 (t, *J* = 7.0 Hz, 3H). Elem. Anal. Calcd. for $C_{50}H_{37}N_3O_4S_6 \bullet 1H_2O$: C 62.94%, H 4.12%, N 4.40%; found C 62.92%, H 3.92%, N 4.04%.

TT-b-03. **5c** (87 mg, 0.1 mmol) was dissolved in CHCl$_3$ (7 mL) then cyanoacetic acid (85 mg, 1.0 mmol) and piperidine (93 mg, 1.1 mmol) were added and the mixture was refluxed for 8 h. The mixture was concentrated and diluted with 10% HCl aqueous solution (15 mL). The formations of a precipitate were observed and filtered under reduced pressure and washed with water (20 mL). The product **TT-b-03** was recovered as dark solid (60 mg, 60%) ^1H NMR (500 MHz, DMSO) δ_H 8.46 (s, 2H), 8.46 (s, 2H), 8.23 (s, 2H), 7.94 (s, 11H), 7.69 (d, *J* = 8.3 Hz, 4H), 7.50 (d, *J* = 8.6 Hz, 2H), 7.23 (d, *J* = 8.2 Hz, 1H), 7.14 m, 6H), 6.62 (s, 1H), 6.57 (s,

1H), 3.98 (t, J = 5.7 Hz, 4H), 1.76-1.60 (m, 4H), 1.34-1.24 (m, 8H), 0.89 (t, J = 6.9 Hz, 3H), 0.82 (t, J = 6.9 Hz, 3H). Elem. Anal. Calcd. for $C_{56}H_{49}N_3O_6S_4 \cdot 3H_2O$: C 64.53%, H 5.32%, N 4.17%; found C 64.17%, H 5.07%, N 4.17%.

Preparation of DSSCs.

DSSCs have been prepared to adapt a procedure reported in the literature.[21] In order to exclude metal contamination all of the containers were in glass or Teflon and were treated with EtOH and 10 % HCl prior to use. Plastic spatulas and tweezers have been used throughout the procedure. FTO glass plates were cleaned in a detergent solution for 15 min using an ultrasonic bath, rinsed with pure water and EtOH. After treatment in a UV-O_3 system for 18 min, the FTO plates were treated with a freshly prepared 40 mM aqueous solution of $TiCl_4$ for 30 min at 70 °C and then rinsed with water and EtOH. A transparent layer of 0.20 cm^2 was screen-printed using Dyesol 18NR-T TiO_2 paste described above. The coated films were thermally treated at 125 °C for 6 min, 325 °C for 10 min, 450 °C for 15 min, and 500 °C for 15 min. The heating ramp rate was 5 - 10 °C/min. The sintered layer was treated again with 40 mM aqueous $TiCl_4$ (70 °C for 30 min), rinsed with EtOH and heated at 500 °C for 30 min. After cooling down to 80 °C the TiO_2 coated plate was immersed into a solution of the dye for 5 h at room temperature in the dark. Counter electrodes were prepared according to the following procedure: a 1-mm hole was made in a FTO plate, using diamond drill bits. The electrodes were then cleaned with a detergent solution for 15 min using an ultrasonic bath, 10% HCl, and finally acetone for 15 min using an ultrasonic bath. After thermal treatment at 500 °C for 30 min, a drop of 5 x 10^{-3} M solution of H_2PtCl_6 in EtOH was added on the cold FTO and the thermal treatment at 500 °C for 30 min repeated. The dye adsorbed TiO_2 electrode and Pt-counter electrode were assembled into a sealed sandwich-type cell by heating with a hot-melt ionomer-class resin (Surlyn 30-μm thickness) as a spacer between the electrodes. A drop of the electrolyte solution was added to the hole and introduced inside the cell by vacuum backfilling. Finally, the hole was sealed with a sheet of Surlyn and a cover glass. A reflective foil at the back side of the counter electrode was taped to reflect unabsorbed light back to the photoanode.

Conflicts of interest

There are no conflicts to declare.

Acknowledgements

Notes and references

1   X. Yang, M. Yanagida and L. Han, *Energy Environ. Sci.*, 2013, **6**, 54-66.

2   B. O'Regan and M. Gratzel, *Nature*, 1991, **353**, 737-740.

3   A. Yella, H.-W. Lee, H. N. Tsao, C. Yi, A. K. Chandiran, M. K. Nazeeruddin, E. W.-G. Diau, C.-Y. Yeh, S. M. Zakeeruddin and M. Grätzel, *Science*, 2011, **334**, 629-634.

4   D. H. Lee, M. J. Lee, H. M. Song, B. J. Song, K. D. Seo, M. Pastore, C. Anselmi, S. Fantacci, F. De Angelis, M. K. Nazeeruddin, M. Gräetzel and H. K. Kim, Dyes Pigm., 2011, 91, 192-198.

5   Z. Yao, M. Zhang, H. Wu, L. Yang, R. Li and P. Wang, *J. Am. Chem. Soc.*, 2015, **137**, 3799-3802.

6   K. Kakiage, Y. Aoyama, T. Yano, K. Oya, T. Kyomen and M. Hanaya, *Chem. Commun.*, 2015, **51**, 6315-6317.

7   A. Abbotto, V. Leandri, N. Manfredi, F. De Angelis, M. Pastore, J. H. Yum, M. K. Nazeeruddin and M. Gratzel, *Eur. J. Org. Chem.*, 2011, 6195-6205.

8   Y. Hong, J.-Y. Liao, J. Fu, D.-B. Kuang, H. Meier, C.-Y. Su and D. Cao, *Dyes Pigm.,* 2012, **94**, 481-489.

9   A. Abbotto, N. Manfredi, C. Marinzi, F. De Angelis, E. Mosconi, J. H. Yum, X. X. Zhang, M. K. Nazeeruddin and M. Gratzel, *Energy Environ. Sci.,* 2009, **2**, 1094-1101.

10 J. Gong, K. Sumathy, Q. Qiao and Z. Zhou, *Renew. Sust. Energ. Rev.*, 2017, **68**, 234-246.

11 Z. Ning and H. Tian, *Chem. Commun.,* 2009, 5483-5495.

12 A. Mahmood, *Solar Energy*, 2016, **123**, 127-144.

13 G. Zhang, H. Bala, Y. Cheng, D. Shi, X. Lv, Q. Yu and P. Wang, *Chem. Comm.,* 2009, 2198-2200.

14 X. Jiang, K. M. Karlsson, E. Gabrielsson, E. M. J. Johansson, M. Quintana, M. Karlsson, L. Sun, G. Boschloo and A. Hagfeldt, *Adv. Funct. Mater.,* 2011, **21**, 2944-2952.

15 N. Manfredi, B. Cecconi and A. Abbotto, *Eur. J. Org. Chem.*, 2014, 7069-7086.

16 Z. Ning, Y. Fu and H. Tian, *Energy Environ. Sci.*, 2010, **3**, 1170-1181.

17 T. Daeneke, A. J. Mozer, T. H. Kwon, N. W. Duffy, A. B. Holmes, U. Bach and L. Spiccia, *Energy Environ. Sci.,* 2012, **5**, 7090-7099.

18 Y. Luo, D. Li and Q. Meng, *Adv. Mater.,* 2009, **21**, 4647-4651.

19 A. Listorti, B. O'Regan and J. R. Durrant, *Chem. Mater.*, 2011, **23**, 3381-3399.

20 B. A. Gregg, F. Pichot, S. Ferrere and C. L. Fields, *J. Phys. Chem. B*, 2001, **105**, 1422-1429.

21 F. Fabregat-Santiago, G. Garcia-Belmonte, I. Mora-Sero and J. Bisquert, *Phys. Chem. Chem. Phys.,* 2011, **13**, 9083-9118.

22 J. Bisquert, F. Fabregat-Santiago, I. Mora-Seró, G. Garcia-Belmonte and S. Giménez, *J. Phys. Chem. C*, 2009, **113**, 17278-17290.

23 J. Halme, P. Vahermaa, K. Miettunen and P. Lund, *Adv. Mater.*, 2010, **22**, E210-E234.

24 Y. Hua, S. Chang, J. He, C. S. Zhang, J. Z. Zhao, T. Chen, W. Y. Wong, W. K. Wong and X. J. Zhu, *Chem. Eur. J.*, 2014, **20**, 6300-6308.

25 A. Mishra, M. K. Fischer and P. Bauerle, *Angew Chem Int Ed*, 2009, **48**, 2474-2499.

26 Z. Sun, M. Liang and J. Chen, *Acc. Chem. Res.,* 2015, **48**, 1541-1550.

27 L. Shi, C. He, D. Zhu, Q. He, Y. Li, Y. Chen, Y. Sun, Y. Fu, D. Wen, H. Cao and J. Cheng, *J. Mater. Chem.,* 2012, **22**, 11629-11635.

28 S. Alesi, F. Di Maria, M. Melucci, D. J. Macquarrie, R. Luque and G. Barbarella, *Green Chemistry*, 2008, **10**, 517-523.

29 J.-H. Yum, T. W. Holcombe, Y. Kim, J. Yoon, K. Rakstys, M. K. Nazeeruddin and M. Gratzel, *Chem. Commun.*, 2012, **48**, 10727-10729.

30 J. O. M. Bockris and S. U. M. Khan, *Surface Electrochemistry - A Molecular Level Approach*, Springer US, New York, NY, USA, 1993.

31 N. Agarwal, C. H. Hung and M. Ravikanth, *Tetrahedron*, 2004, **60**, 10671-10680.

32 J. Tauc, *Mater. Res. Bull.*, 1968, **3**, 37-46.

33 E. M. Barea, V. Gónzalez-Pedro, T. Ripollés-Sanchis, H.-P. Wu, L.-L. Li, C.-Y. Yeh, E. W.-G. Diau and J. Bisquert, *J. Phys. Chem. C,* 2011, **115**, 10898-10902.

34 X. Jiang, T. Marinado, E. Gabrielsson, D. P. Hagberg, L. Sun and A. Hagfeldt, *J. Phys. Chem. C,* 2010, **114**, 2799-2805.

35 C.-Y. Chen, M. Wang, J.-Y. Li, N. Pootrakulchote, L. Alibabaei, C.-h. Ngoc-le, J.-D. Decoppet, J.-H. Tsai, C. Grätzel, C.-G. Wu, S. M. Zakeeruddin and M. Grätzel, *ACS Nano*, 2009, **3**, 3103-3109.

36 S. Ito, M. K. Nazeeruddin, P. Liska, P. Comte, R. Charvet, P. Pechy, M. Jirousek, A. Kay, S. M. Zakeeruddin and M. Gratzel, *Prog Photovoltaics*, 2006, **14**, 589-601.

37 T. Markvart and L. Castañer, *Solar Cells*, Elsevier Science, Oxford, 2005.

38 Dye Sensitized Solar Cells, CRC Press, Boca Raton, FL, USA, K.Kalyanasundaram edn., 2010.

39 M. Grätzel, *Acc. Chem. Res*., 2009, **42**, 1788-1798.

40 A. Hagfeldt, G. Boschloo, L. Sun, L. Kloo and H. Pettersson, *Chem. Rev.,* 2010, **110**, 6595-6663.

41 M. K. Nazeeruddin, E. Baranoff and M. Grätzel, *Solar Energy*, 2011, **85**, 1172-1178.

42 H. J. Snaith, *Adv. Funct. Mater*., 2010, **20**, 13-19.

43 V. Trifiletti, R. Ruffo, C. Turrini, D. Tassetti, R. Brescia, F. Di Fonzo, C. Riccardi and A. Abbotto, *J. Mater. Chem. A*, 2013, **1**, 11665-11673.

44 A. Orbelli Biroli, F. Tessore, V. Vece, G. Di Carlo, P. R. Mussini, V. Trifiletti, L. De Marco, R. Giannuzzi, M. Manca and M. Pizzotti, *J. Mater. Chem. A*, 2015, **3**, 2954-2959.

45 A. Smets, K. Jäger, O. Isabella, R. v. Swaaij and M. Zeman, *Solar Energy Physics of photovoltaic conversion technologies and systems*, UIT, Cambridge, UK, 2016.

University of Milano-Bicocca

Via R. Cozzi 53, I-20125 Milano, Italy
http://www.mater.unimib.it

Milano, 30 December 2017

Dear Prof. Mir Wais Hosseini,
Editor-in-chief
New Journal of Chemistry

Please find herewith enclosed the manuscript:

"Performance enhancement of dye-sensitized solar cell by peripheral aromatic and heteroaromatic functionalization in di-branched organic sensitizers"

by N. Manfredi,[*] V. Trifiletti, F. Melchiorre, G. Giannotta, P. Biagini,[*] and A. Abbotto.[*]

that we would like to submit to *New Journal of Chemistry* for publication as a full paper.

This work presents the detailed investigation of a series of organic dyes as sensitizers for dye-sensitized solar cells (DSSC). In particular, we focussed on the peripheral functionalization of a class of di-branched dyes, a molecular geometry that we have introduced in the DSSC field a few years ago (Ref. 10) and then adopted by other researchers (review: Ref 16) as a successful strategy for DSSC dye sensitizers.

The molecular di-branched architecture D-(π-A)$_2$ has been based on the triphenylamine core as a donor D group and the cyanoacrylic moiety as an acceptor-anchoring group, using a thieno[3,2-*b*]thiophene as π spacer, previously used in efficient DSSC sensitizers. Starting from this basic configuration, a number of auxiliary donor groups have been selected and introduced as peripheral functionalization on the donor fragment in order to enhance relevant molecular (e.g., light harvesting) and device (power conversion efficiency, PCE) properties.

The new compounds have been investigated in their optical and photovoltaic properties in comparison with the unsubstituted compound **TT-b-00** as a reference system. Indeed optical (red shift and molar absorptivity) and PCE were significantly improved compared to the reference dye. The measured photovoltaic efficiency (> 6%) is not top ranked in absolute terms but compares well with the benchmark sensitizer N719 used under the same conditions. In fact, we focussed our study on the fundamental understanding of dye working principles. Accordingly, DSSCs have been realized with the aim of simplifying the architecture in a single layer device, which is less performing than opaque double layer configuration but allowed us to study in deeper details the relevant interface phenomena. The photovoltaic investigation highlighted the superior photovoltaic properties of the substituted **TT-b-02** dye, bearing the 5-hexyl-2,2'-bithienyl fragment as auxiliary donor group. We have found a more efficient interaction between dye-sensitized TiO$_2$ and the liquid electrolyte.

We thus believe that the new dyes might provide a new design strategy to improve general performances in large area DSSCs of industrial relevance (participating as co-authors in this work), a sector where the critical interface between the optically active layer and the electrolyte is still a challenging issue.

Recently, the *Journal* has devoted much attention to organic molecules and materials for photovoltaics with PCE comparable to those reported in our submitted manuscript (see, for instance, the following recent examples: S. Ashraf, J. Akhtar, H. M. Siddiqi and A. El-Shafei, *New J. Chem.*, 2017, **41**, 6272-6277; I. Pecnikaj, D. Minudri, L. Otero, F. Fungo, M. Cavazzini, S. Orlandi and G. Pozzi, *New J. Chem.*, 2017, **41**, 7729-7738; R.-Y. Huang, Y.-H. Chiu, Y.-H. Chang, K.-Y. Chen, P.-T. Huang, T.-H. Chiang and Y. J. Chang, *New J. Chem.*, 2017, **41**, 8016-8025; Y. Li, P. Song, Y. Yang, F. Ma and Y. Li, *New J. Chem.*, 2017, **41**, 12808-12829; S. Erten-Ela, Y. Ueno, T. Asaba and Y. Kubo, *New J. Chem.*, 2017, **41**, 10367-10375). We thus trust that our results should be of interest to the many readers of the *New Journal of Chemistry* involved in this topic.
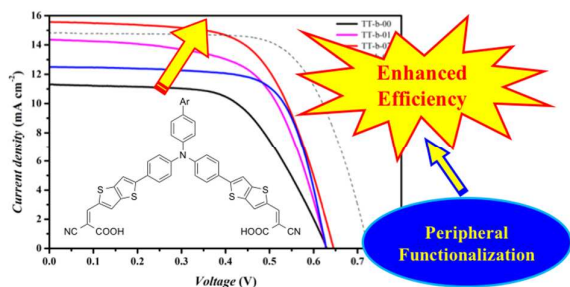
Best regards,

Alessandro Abbotto, Norberto Manfredi and Paolo Biagini

Performance enhancement of dye-sensitized solar cell by peripheral aromatic and heteroaromatic functionalization in di-branched organic sensitizers

N. Manfredi, V. Trifiletti, F. Melchiorre, G. Giannotta, P. Biagini, and A. Abbotto.

Table of contents entry

Suppression of back reaction and enhanced photoinduced intramolecular electron transfer through peripheral functionalization of triphenylamino based dibranched donor-acceptor dyes.

Performance enhancement of dye-sensitized solar cell by peripheral aromatic and heteroaromatic functionalization in di-branched organic sensitizers

N. Manfredi, V. Trifiletti, F. Melchiorre, G. Giannotta, P. Biagini, and A. Abbotto.

Electronic Supplementary Information
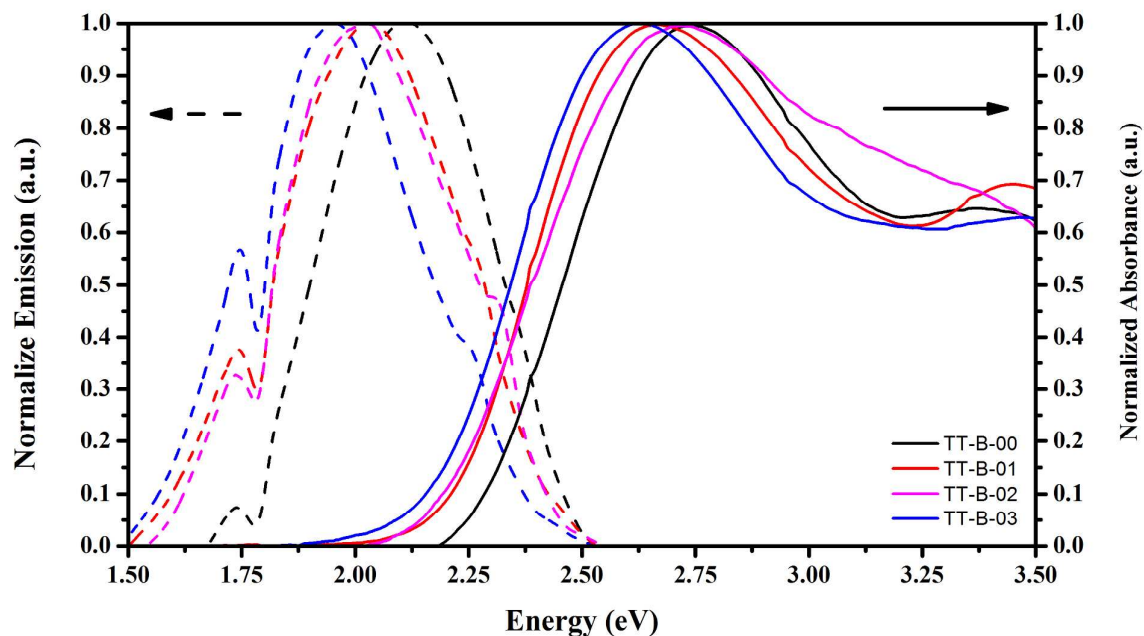
Table of contents

Figure S1. Normalized absorption (solid line) and emission (dashed line) spectra of the investigated dyes in EtOH solution.
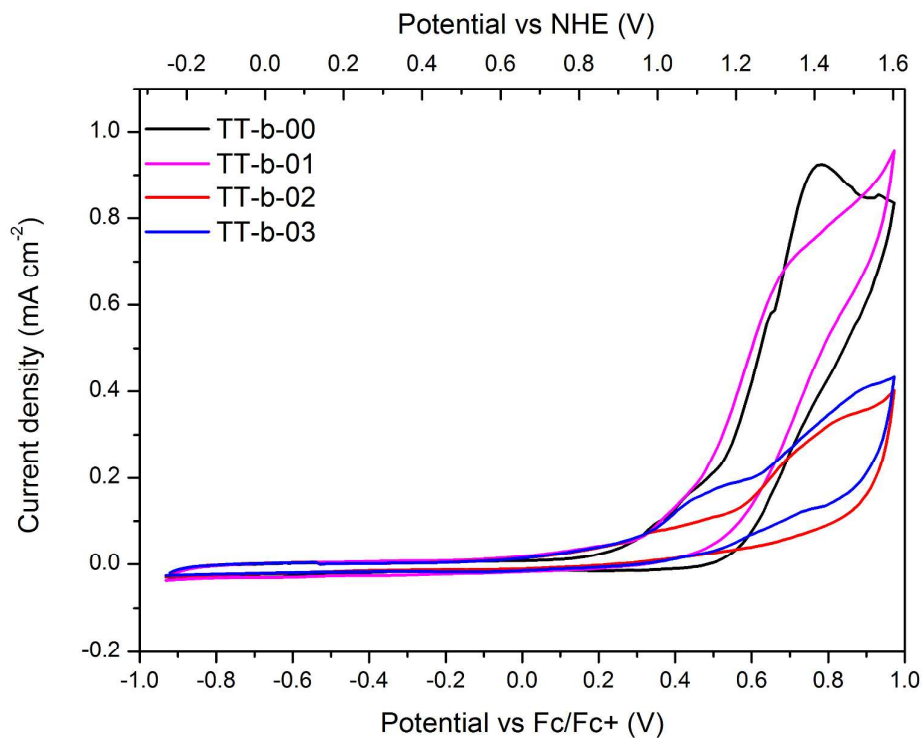

Figure S2. Cyclic voltammetry (CV) plots of the investigated dyes in TBABF$_4$ 0.1 M in DMF solution.

Table S1: Main photovoltaic parameters of DSSCs based on the di-branched sensitizer **TT-b-02**, varying the electrolyte and the chenodeoxycholic acid (**CDCA**) amount in the 2×10^{-4} M dye solution.

Electrolyte	CDCA (M)	J_{sc} (mA cm^{-2})	V_{oc} (mV)	FF	PCE (%)
Z959 [a]	0	14.0	624	0.70	6.1
Z960 [b]	0	12.7	664	0.68	5.7
Z959 [a]	2×10^{-4}	15.9	663	0.59	6.2
Z960 [b]	2×10^{-4}	15.6	645	0.62	6.3
Z959 [a]	2×10^{-3}	12.9	628	0.71	5.8
Z960 [b]	2×10^{-3}	12.8	678	0.70	6.1
Z959 [a]	2×10^{-2}	12.6	619	0.72	5.6
Z960 [b]	2×10^{-2}	12.9	678	0.71	6.2

[a] 1.0 M DMII, 0.03 M I$_2$, 0.1 M GSCN, 0.5 M TBP in ACN/VN=85/15; [b] 1.0 M DMII, 0.03 M I$_2$, 0.05 LiI, 0.1 M GSCN, 0.5 M TBP in ACN/VN=85/15.

^{1}H and ^{13}C NMR spectra

3764.75
3756.08
3707.91
3671.87
3666.68
3664.39
3656.03
3648.50
3624.46
3619.33
3593.12
3585.56
3571.00
3562.35
3555.50
3548.25
3541.77

500 MHz in CDCl$_3$

500 MHz in DMSO-d_6

500 MHz in DMSO-d_6

125 MHz in DMSO-d_6

500 MHz in CDCl$_3$

125 MHz in CDCl₃

500 MHz in CDCl₃

500 MHz in CDCl₃

500 MHz in DMSO-d₆

500 MHz in DMSO-d_6

500 MHz in DMSO-d_6

500 MHz in DMSO-d_6